# ANGULAR DISTRIBUTIONS OF SULFUR ATOMS IN THE 3p $^3P_J$ and 3p $^1D$ STATES FROM TWO-PHOTON DISSOCIATION OF CARBON DISULFIDE

Masahiro KAWASAKI [1], Hiroyasu SATO
*Chemistry Department of Resources, Faculty of Engineering, Mi'e University, Tsu 514, Japan*

Shuichiro KOBAYASHI and Tatsuo ARIKAWA
*Department of Applied Physics, Faculty of Technology, Tokyo University of Agriculture and Technology, Koganei 184, Japan*

Received 26 October 1987; in final form 8 January 1988

A molecular beam of carbon disulfide was photodissociated at 288–292 and 308–309 nm (a one-color, multiphoton dissociation). The angular distributions of sulfur atoms were measured in the S (3p $^3P_J$) and (3p $^1D_2$) states. Both S ($^1D$) and ($^3P_J$) fragments have anisotropic distributions for the two-photon dissociation.

## 1. Introduction

$CS_2$ is one of the triatomic molecules whose photodissociation dynamics have been studied by time-of-flight mass spectroscopy [1,2], laser-induced fluorescence [3], VUV absorption [4] and also diode laser absorption [5] techniques. It has been recognized that there are two primary processes for one-photon photodissociation of $CS_2$ in the UV region. One is the spin-allowed process from the optically prepared state; the other is the spin-forbidden process which becomes partially allowed by large spin–orbit interactions of two sulfur atoms in $CS_2$:

$$CS_2 + \hbar\omega \rightarrow CS_2^* ,$$

$$CS_2^* \rightarrow CS\,(X\,^1\Sigma) + S\,(^3P_J)\,, \qquad \text{(I)}$$

$$CS_2^* \rightarrow CS\,(X\,^1\Sigma) + S\,(^1D)\,. \qquad \text{(II)}$$

When the photon energy is increased, CS can be electronically excited. At ≈ 8 eV the intense Rydberg features of $CS_2$ lying to shorter wavelengths correlate directly with CS ($a\,^3\Pi$)+S ($^3P$) and once the threshold at 158 nm has been crossed it is in this region that the quantum yield of CS ($a\,^3\Pi$) rises steeply in the one-photon dissociation of $CS_2$ [6]. The energetics of $CS_2$ dissociation are shown in table 1. There are several dissociation pathways which generate S fragments in the $^3P_J$, $^1D_2$, and $^1S_0$ states. These pathways can be attained by two-photon absorption of UV laser light via a real intermediate state of $CS_2$. The two-photon dissociation at 308 nm (4.0 eV) via the V system of $CS_2$ ($^1B_2$) has been reported for the translational energy and angular distributions of the sulfur photofragments in the S ($^3P_2$) state [8]:

Table 1
Theshold energies (eV) of primary photodissociative processes for $CS_2$ [a)]

| CS | S | | |
|---|---|---|---|
| | $^3P_2$ | $^1D_2$ | $^1S_0$ |
| $X\,^1\Sigma$ | 4.46(I) | 5.61(II) | 7.21(IV) |
| $a\,^3\Pi$ | 7.88(III) | 9.03 | 10.63 |
| $a'\,^3\Sigma^+$ | 8.32 | 9.47 | |
| $d\,^3\Delta$ | 8.88 | 10.03 | |
| $e\,^3\Sigma^-$ | 9.25 | 10.40 | |
| $A\,^1\Pi$ | 9.27 | | |

$\Delta E\,(^3P_1-{}^3P_2) = 0.049$ eV
$\Delta E\,(^3P_0-{}^3P_2) = 0.071$ eV

[a)] Ref. [7]. Numbers in parentheses denote the primary photodissociation processes, see text.

---

[1] Present address: Research Institute of Applied Electricity, Hokkaido University, Sapporo 060, Japan.

0 009-2614/88/$ 03.50

$$CS_2(\tilde{X}\,^1\Sigma_g) \xrightarrow{\hbar\omega} CS_2^*\,(^1B_2) \xrightarrow{\hbar\omega} CS_2^{**}\,(^1A_1)\,,$$

$$CS_2^{**} \rightarrow CS\,(X\,^1\Sigma, a\,^3\Pi) + S\,(^3P_2)\,.$$

The angular distribution of S ($^1$D) has not been reported although the formation of S ($^1$D) is confirmed in the VUV one-photon dissociation [9]. If the dissociating species is the same for both S ($^3P_2$) and S ($^1$D) fragments, the angular distributions would have the same anisotropic parameters for both fragments. In this paper, we report on measurement of angular distributions of S ($^3P_J$) and S ($^1$D) generated in the two-photon dissociation via the $^1B_2$ state since the $\beta$ values contain information on lifetimes, molecular structures and symmetries of dissociating states.

## 2. Experimental

The sulfur atomic photofragments were generated and ionized by one-color multiphoton dissociation and ionization. The angular distributions of ions were measured by a homemade mass spectrometer that has theoretically a perfect focusing property as has been described elsewhere [10,11]. Briefly, the perfect focusing property was realized by the combination of a uniform magnetic field with a three-dimensional quadrupole electrostatic field. The ions of a certain mass number generated in one focusing point of the electrostatic field reach the other focusing point irrespective of their initial velocity vectors. For mass analysis, the mass number was selected by changing the strength of the electric field. The detector has a slit for spatial resolution. The angular distribution of the photofragments was measured by changing the laboratory angle $\Theta$ between the directions of the detector axis and the electric vector of the dye laser light (Lambda Physik FL 2002) with mass number fixed at $m/e = 32$. The effusive molecular beam of $CS_2$ was introduced through a needle (0.3 mm diameter) near the focusing point where the laser beam was focused by a lens of $f = 15$ cm. The maximum laser intensity is estimated ≈30 GW/cm$^2$ assuming a Gaussian profile of the laser beam. The polarization of the laser beam was changed from linearly polarized to circularly polarized by retardation plates.

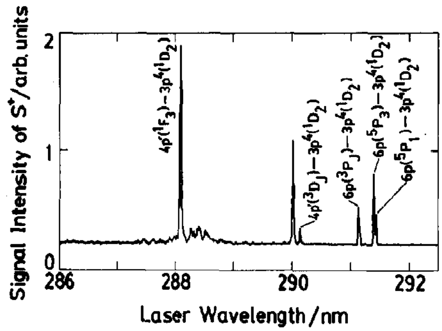

Fig. 1. Multiphoton-ionization spectrum of S atoms generated in multiphoton dissociation of $CS_2$ at 286–292 nm. Table 2 shows assignments of the two-photon transitions of sulfur atoms.

## 3. Results

A photon of wavelength longer than 277.7 nm contains insufficient energy to dissociate a $CS_2$ molecule. As the dye laser was scanned over the two wavelength ranges, $\lambda = 288$–292 nm and 308–311 nm, sulfur atoms were generated via two-photon dissociation of $CS_2$. Successive resonance-enhanced photoionization (MPI) in sulfur photofragments occurred by the 2+1 three-photon (two to resonance) ionization in the 3 $^3P_J$ and 3 $^1D_2$ states as shown in figs. 1 and 2. These photofragments can be generated by two-photon absorption of the same laser photons:

$$CS_2 \xrightarrow{2\hbar\omega} CS + S\,(^3P_J, {}^1D)\,,$$

$$S\,(^3P_J, {}^1D) \xrightarrow{2\hbar\omega} S^* \xrightarrow{\hbar\omega} S^+\,,$$

where S* denotes an electronically excited sulfur atom. At $\lambda = 288$–292 nm, the MPI spectrum of fig.

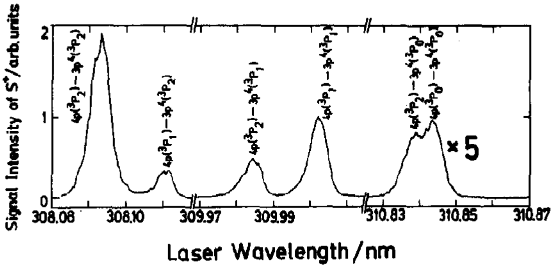

Fig. 2. Multiphoton-ionization spectrum of S atoms generated in multiphoton dissociation of $CS_2$ at 308–311 nm. Table 3 shows relative intensities of $J''$ levels in S (3p $^3P_{J''}$).

Table 2
Assignments of two-photon transitions of S atoms in two-photon dissociation of $CS_2$ with anisotropy parameters

| $\lambda$ (nm) | | Two-photon transition | $\beta_2$ [a] | $n$ [b] | $\Omega$ [c] |
|---|---|---|---|---|---|
| air | vacuum | | | | |
| 288.11 | 288.19 | $4\,^1F_3$–$3\,^1D_2$ | $0.88\pm0.07$ | $3.1\pm0.1$ | 0.5 |
| 290.02 | 290.10 | ? –$3\,^1S_0$ | $1.13\pm0.16$ | $5.1\pm0.1$ | 0.2 |
| 291.14 | 291.22 | $6\,^3P_0$–$3\,^1D_2$ | $0.81\pm0.08$ | $3.9\pm0.1$ | 0.6 |
| 291.39 | 291.47 | $6\,^5P_3$–$3\,^1D_2$ | $0.88\pm0.08$ | $3.4\pm0.1$ | 0.6 |
| 291.40 | 291.49 | $6\,^5P_1$–$3\,^1D_2$ | $0.88\pm0.08$ | $3.3\pm0.1$ | 0.3 |
| 308.10 | 308.20 | $4\,^3P_2$–$3\,^3P_2$ | $0.54\pm0.07$ | $3.0\pm0.1$ | – |
| 310.01 | 310.10 | $4\,^3P_2$–$3\,^3P_1$ | $0.52\pm0.07$ | $2.8\pm0.1$ | – |
| 310.84 | 310.94 | $4\,^3P_2$–$3\,^3P_0$ | $0.52\pm0.07$ | $3.2\pm0.1$ | – |
| 308 [d] | | $4\,^3P_2$–$3\,^3P_2$ | $0.67\pm0.12$ | | |

[a] Anisotropy parameters in eq. (1). $\beta_4$ values were found to be zero.
[b] Power index $n$ is defined by $I_{\mathrm{ion}} \propto (I_{\mathrm{laser}})^n$.
[c] Intensity ratio $I_c/I_l$ where $I_c$ and $I_l$ are the signal intensity for circularly and linearly polarized laser light respectively.
[d] Untuned XeCl excimer laser light [8]. S ($^3P_2$) is generated by primary process (I).

1 is assigned to the transitions from S ($3\,^1D$) except for the line at 290.02 nm. The assignments of the two-photon transitions of S atoms are summarized in table 2. The MPI excitation spectra at 308–311 nm were observed in more detail for the transition of $4\,^3P_2 \leftarrow 3\,^3P_{J''}$. The relative population of the $J''$ levels were obtained using the two-photon absorption cross sections reported by Brewer et al. [12]. The results are summarized in table 3. The prior expectation for this branching ratio [13] is given by

$$g(^3P_J)\,[E_{\mathrm{AVL}}(^3P_J)]^{5/2}/g(^3P_{J'})\,[E_{\mathrm{AVL}}(^3P_{J'})]^{5/2},$$

which is approximated by $(2J+1)/(2J'+1)$, while the ratios obtained experimentally are only 1.2–1.4. The $J''$ population distributions obtained are not statistical. This result suggests that the formation of the $J''$ levels may not be a statistical process like the predissociation via the hot $CS_2$ molecule.

Table 3
Relative intensity of S ($^3P_J$)

| Two-photon transition | Relative signal intensity, $I$ | $I/\sigma$ [a] |
|---|---|---|
| $4\,^3P_2$–$3\,^3P_2$ | 13.6 | 1.2 |
| $4\,^3P_2$–$3\,^3P_1$ | 3.3 | 1.4 |
| $4\,^3P_2$–$3\,^3P_0$ | 1 | 1 |

[a] Two-photon absorption cross section $\sigma$ is adopted from ref. [12].

By choosing appropriate wavelengths for S ($^3P_J$, $^1D$), the intensity of $S^+$ was measured as a function of $\Theta$. An example is shown in fig. 3. In these experiments, the laser power was reduced until the $\beta$ values reached asymptotic values in order to avoid the reduction of the $\beta$ values caused by saturation effects. The experimentally obtained angular distribution is close to the one obtained in the center-of-mass angular distribution $f(\theta)$ that is given by the following equation;

$$f(\theta) \propto 1 + \beta_2 P_2(\cos\theta) + \beta_4 P_4(\cos\theta)\,, \qquad (1)$$

where $P_l(\cos\theta)$ is the $l$th degree Legendre polynomial [14]. The curve drawn through the set of data of

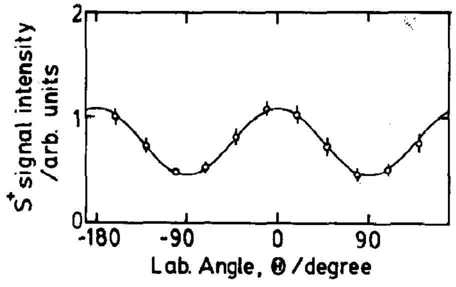

Fig. 3. Angular distribution of S ($^1D$) photofragments from $CS_2$ multiphoton dissociation at 288.10 nm. The solid line is the least-squares fit of the data with eq. (1) for $\beta_2 = 0.88$ and $\beta_4 = 0$.

fig. 3 shows the least-squares fit of eq. (1) to the data. Other sets of data were also analyzed by this method. The $\beta_2$ values were positive while the $\beta_4$ values were found to be zero for all sets of data. $\beta_2$ values obtained are summarized in table 2. The $\beta_2$ value for S ($^3P_2$) generated in the 308 nm photodissociation has been previously reported to be 0.67 by the MPI TOF method [8]. Compared with fig. 6 of ref. [8], fig. 3 of the present work is much improved in the S/N ratios because of the high sensitivity of our perfect focusing mass spectrometer. Although there is some discrepancy between the previously reported value of $\beta_2=0.67\pm0.12$ and the present work of $\beta_2=(0.52-0.54)\pm0.07$, it is safe to say that the $\beta_2$ values of S ($^3P_J$) are $\approx 0.6$ for the two-photon dissociation of $CS_2$ at 308–318 nm and less than those ($\approx 0.9$) of S ($^1D$) obtained in the two-photon dissociation of $CS_2$ at 288–292 nm.

## 4. Discussion

The intense and complicated absorption system of $CS_2$ in the region of 290–330 nm is called the V system. This V system is due to the transition from the ground $^1\Sigma_g^+$ state to the $^1B_2$ state ($\angle SCS=131°$) that fluoresces with unit quantum yield [15]. Douglas and Milton [16] have studied the pronounced Zeeman effect of the absorption bands ($^1B_2 \leftarrow \tilde{X}\,^1\Sigma_g^+$) of $CS_2$ and have shown that it can be understood if the observed $^1B_2$ state is a component of a $^3A_2$ state. The lowest $^3A_2$ state was detected by the technique of resonance-enhanced MPI at 361–371 nm [17]. This singlet–triplet transition is reported to have an oscillator strength of $\approx 10^{-7}$ [18]. Thus, the singlet–triplet coupling seems to be weak in $CS_2$ at $\approx 365$ nm. However, Kanamori and Hirota [5] have reported that the spin-forbidden triplet channel (I) makes a significant contribution to the one-photon dissociation of $CS_2$ at 193 nm. The branching ratio of channels (I) and (II) is reported to be 1–0.25 [1,2,5] although the prior distribution [13] predicts that the ratio is 14.4. The intersystem crossing process seems to be a bottleneck one for yielding the S ($^3P_J$) fragments. Although it was difficult to determine this ratio in the present work, the signal intensities of both S ($^3P$) and S ($^1D$) were comparable in the present experiment.

In the present multi-photon dissociations in the UV region, the $\beta_4$ values of eq. (1) were found to be zero as described above. This result implies that the dissociation is due to the two-photon absorption of $CS_2$ via the real intermediate $^1B_2$ state:

$$CS_2+\hbar\omega \to CS_2^*(^1B_2)\,,$$

$$CS_2^*(^1B_2)+\hbar\omega \to CS_2^{**} \to CS+S\,(^3P_J,\,^1D)\,.$$

In the two-photon dissociation via a real and stable state the angular distribution must be represented by eq. (1) with $\beta_4=0$. If $CS_2$ absorbed three UV photons, $\beta_4$ would not be zero because the final two-photon absorption occurs via a real and dissociative intermediate state. Kawasaki et al. [8] have reported that $\beta_4$ was not zero or the $P_4(\cos\theta)$ term contributed to $f(\theta)$ for the two-photon dissociation of $NO_2$ via the real and dissociative intermediate state.

The two-photon energies for the photolysis at $\approx 290$ and $\approx 308$ nm are 8.5 and 8.0 eV, respectively. Table 1 shows that the following primary processes are energetically possible,

$$CS_2 \begin{cases} \to CS\,(X\,^1\Sigma) + S\,(^3P_J)\,, & \text{(I)} \\ \to CS\,(X\,^1\Sigma) + S\,(^1D_2)\,, & \text{(II)} \\ \to CS\,(a\,^3\Pi) + S\,(^3P_J)\,, & \text{(III)} \\ \to CS\,(X\,^1\Sigma) + S\,(^1S_0)\,. & \text{(IV)} \end{cases}$$

In the one-photon photolysis in the UV region, processes (I), (II), and (III) have been reported [1–6]. We have previously reported that the contribution of the spin-allowed process (III) is comparable to that of the spin-forbidden process (I), based on the TOF spectrum of the S ($^3P$) fragments from two-photon dissociation at 308 nm [8]. The spin-forbidden process (I) contributes to the S ($^3P_2$) formation through the bottlenecking intersystem crossing to the triplet repulsive state from the photoprepared singlet state as has been reported for the one-photon dissociation [1,2]. Elementary kinetics considerations will show that while a bottleneck such as that invoked will affect the yields of the various channels, the production rate of every species will be the same, determined by the sum of the rates through all channels. The rate can be estimated from the $\beta$ values, molecular symmetries, and structures as will be described later. In brief, the smaller decay rate, the smaller is the $\beta$ value if the molecular structure is not changed. In the present work the $\beta_2$ values for S ($^3P_J$) are smaller than those for S ($^1D_2$) as shown in table 2. If a single photo-prepared state is the originating excited $CS_2$ state for S ($^3P$) and S ($^1D$) production, then the only way for the $\beta$ values of S ($^3P$) to differe from those of S ($^1D$) is for the molecular structure of the triplet dissociating state to differ from that of the singlet one:

$$CS_2 \xrightarrow{\hbar\omega} CS_2^* \, (^1B_2) \xrightarrow{\hbar\omega} CS_2^{**} \, (\text{singlet}) \, ,$$

$$CS_2^{**} \begin{array}{l} \longrightarrow CS_2^* \, (\text{triplet}) \rightarrow CS + S \, (^3P) \, , \\ \longrightarrow CS + S \, (^1D) \, . \end{array}$$

Concerning the symmetries of the dissociating states of $CS_2$, since the first one-photon transition is $^1B_2 \leftarrow \tilde{X} \, ^1A_1$ in $C_{2v}$ approximation, the symmetry-allowed states for the second one-photon absorption are $A_1$, $A_2$, and $B_2$. If the singlet dissociating state retains the structure of the intermediate $^1B_2$ state ($\angle CSC = 131°$), only the $^1A_1 \leftarrow {}^1B_2 \leftarrow \tilde{X} \, ^1A_1$ transition gives a positive $\beta_2$ value according to the following equation [19]:

$$\beta_2 = 2P_2(\cos\chi) \frac{1+\omega^2\tau^2}{1+4\omega^2\tau^2} \, , \tag{2}$$

where $\chi$ is the angle between the transition moment and the dissociation direction, $\omega$ the angular velocity of the parent molecule, and $\tau$ the dissociation lifetime. When the second transition moment lies in the S–S direction, $\chi$ is 24.5° and $\beta_2$ is 1.48. The lifetime estimated is $\approx 0.3$ ps for the S ($^1D$) channel using eq. (2) with $\beta_2$ values in table 2 and $\omega = 2 \times 10^{12}$ s$^{-1}$. The value of $\omega$ is estimated from the relation $\omega = (\pi kT/2I)^{1/2}$, where $I$ is the average of the two large, nearly equal moments of inertia in the $^1B_2$ state of $CS_2$.

At 290.02 nm excitation, the $\beta$ values are larger than those for S ($^1D$). The power dependence is larger than others. In addition the intensity ratio $I_c/I_\ell$ is also different from that for S ($^1D_2$) where $I_c$ is the MPI signal intensity for circularly polarized laser light and $I_\ell$ for linearly polarized one. The atomic transition is not from S ($^1D_2$) nor is clear even from the reported Grotrian energy level diagram [20]. The transition at 290.02 nm may be from a singlet state, probably S ($3\,^1S_0$) generated from process (IV), because the $\beta$ value is larger than for S($^3P_J$) and close to the singlet channel (II).

## Acknowledgement

This work is partly supported by a Grant-in-Aid for Scientific Research from the Ministry of Education, Science, and Culture of Japan.

## References

[1] S.C. Yang, A. Freedmen, M. Kawasaki and R. Bersohn, J. Chem. Phys. 72 (1980) 4058.
[2] V.R. McCrary, R. Lu, D. Zakheim, J. Halpern, J. Russell and W. Jackson, J. Chem. Phys. 83 (1985) 3481.
[3] J.E. Butler, W.S. Drozdoski and J.R. McDonald, Chem. Phys. 50 (1980) 413.
[4] M.C. Addison, R.J. Donovan and C. Fotakis, Chem. Phys. Letters 74 (1980) 58.
[5] H. Kanamori and E. Hirota, J. Chem. Phys. 86 (1987) 3901.
[6] G. Black, R.L. Sharpless and T.G. Slanger, J. Chem. Phys. 66 (1977) 2113.
[7] M.N.R. Ashfold, M.T. McPherson and J.P. Simons, Topics in current chemistry, Vol. 86 (Springer, Berlin, 1979) p. 1.
[8] M. Kawasaki, H. Sato, T. Kikuchi, A. Fukuroda, S. Kobayashi and T. Arikawa, J. Chem. Phys. 86 (1987) 4425.
[9] M.C. Addison, C.D. Byre and R.J. Donovan, Chem. Phys. Letters 64 (1979) 57.
[10] T. Arikawa, Japan. J. Appl. Phys. 2 (1963) 420.
[11] M. Kawasaki, H. Sato, A. Fukuroda, T. Kikuchi, S. Kobayashi and T. Arikawa, J. Chem. Phys. 86 (1987) 4431.
[12] P. Brewer, N. van Veen and R. Bersohn, Chem. Phys. Letters 91 (1982) 126.
[13] R.D. Levine and R.B. Bernstein, Chem. Phys. Letters 29 (1974) 1.
[14] R. Sander and K. Wilson, J. Chem. Phys. 63 (1975) 4242.
[15] H. Kasahara, N. Mikami, M. Ito and S. Iwata, Chem. Phys. 86 (1984) 173.
[16] A.E. Douglas and E.R.V. Milton, J. Chem. Phys. 41 (1964) 357.
[17] R. Rianda, P.J. Moll and A. Kuppermann, Chem. Phys. Letters 73 (1980) 469.
[18] T. Barrow and R.W. Dixon, Mol. Phys. 25 (1979) 137.
[19] C. Jonah, J. Chem. Phys. 55 (1971) 1915.
[20] S. Bashkin and J.O. Stoner Jr., Atomic energy-level and Grotrian diagrams, Vol. 2 (North-Holland, Amsterdam, 1978).